Estimating load condition having caused structure failure and an optimal design taking account of the estimated result

T. Muromaki[1)], K. Hanahara[2)], Y. Tada[2)], S. Kuroda[3)] and T. Fukui[3)]
[1)] *Graduate School of Engineering, Kobe University, Kobe, 657-8501, Japan*
email: muromaki@opt.cs.kobe-u.ac.jp
[2)] *Graduate School of System Informatics, Kobe University, Kobe, 657-8501, Japan*
email: hanahara@cs.kobe-u.ac.jp, tada@cs.kobe-u.ac.jp
[3)] *Martec K. K., Kobe, 650-0046, Japan*
email: kuroda@martec.co.jp, fukui@martec.co.jp

Abstract: In order to improve a design of structure, it is important to know the actual load condition of failed structure. We develop an estimation method of loading conditions based on images of failed structures and an FEM analysis model. Preparing a database that consists of deformation data of the structure corresponding to various load conditions, our system is able to estimate the load conditions that caused structure failure based on the processed images of failed structure samples. Adopting elasto-plastic model of the structure, the magnitude of the load having caused the failure is also estimated in addition to the position and orientation of the critical load. We adopt the EM algorithm to obtain the distribution of the critical load. An optimal design problem that takes account of the distribution of the estimated critical load condition is formulated as a minimization problem with a multi-objective function; the stiffness and the structural weight are also adopted as the evaluation items that make up the objective function. The particle swarm optimization (PSO) is adopted as the optimization algorithm. The approach is applied to crane-hook. The result of estimated critical load distribution and the optimal design based on the load distribution are demonstrated.

Keywords: load estimation; optimal design; database; finite element analysis; EM algorithm; crane-hook.

1. Introduction

Avoiding failure of structure system is one of the most important missions for design engineer of structures. In order to improve an existing structure so that it does not fail, it is important to know the load condition that causes structure failure. Generally, the load condition is identified by integrating the information obtained from the sensor devices; continuous monitoring is essential. However, almost all structures themselves have no information about the load conditions during their service life. In this case, several failure detection methods proposed in the past are not applicable (Quek et al., 2009; Lam and Ng, 2009). It is necessary to estimate the load condition by means of another approach. We develop a load estimation system; this system is applicable to the failed structures having permanent deformation. The system inputs the digital images of failed structures and outputs the estimated probability of the load conditions that caused the failure. The information from the sensor devices is not required. We deal with the failed crane-hooks as a concrete example.

Crane-hook is one of the most useful equipments for suspension work. Recently, excavators having a

5th International Conference on Reliable Engineering Computing (REC 2012)
Edited by M. Vořechovský, V. Sadílek, S. Seitl, V. Veselý, R. L. Muhanna and R. L. Mullen

ISBN 978-80-214-4507-9. Published by Ing. Vladislav Pokorný − LITERA

crane-hook are widely used in construction work sites. One reason is that there are work sites where the crane trucks for suspension work are not available because of the narrowness of the working site; an excavator has superior to a crane truck in general. Another reason is that such an excavator is convenient because they can perform the conventional digging tasks as well as the hanging works mentioned above. Figure 1 shows a sample of excavator with crane-hook and the close-up image of its bucket part where the crane-hook is attached.

Though it has such a convenience, there are cases that the crane-hooks are damaged during some kind of hanging works. Figure 2 shows a typical crane-hook and its damaged sample to be repaired. This type of hook can be used to suspend objects whose weight is up to 2.9t. In Fig. 2, we can see that the locking apparatus, called latch, is left open. From the view point of safety, such failure must be avoided. Improvement of the performance and the service life is important; the real conditions of such suspension tasks in practical environment are, however, still unclear. Therefore, the identification of the cause of failure is one of the key issues for the safety improvement.

Our previous work (Muromaki et al., 2012) gives the estimation of such load conditions in the form of probability distribution. In the study, however, we focused only on the estimation of the load applied position and the direction. We did not estimate the load magnitude. This is because the analysis model is based on the linear deformation theory and the analysis results do not well reflect the significant magnitude of the applied load that causes the permanent deformation as shown in Fig. 2. In the current study, the analysis model is improved so as to be applicable for the permanent deformation. By adding the information of the load magnitude, the failure estimation result becomes more meaningful.

In addition to the load estimation approach, we discuss an optimal design taking account of the estimated result. In order to improve the performance of crane-hook, we formulate the multi-objective optimization problem considering the structural weight and the stiffness. The evaluation of stiffness is performed in terms of the estimated load conditions. The optimization problem is solved by using the particle swarm optimization (PSO).

The outline of this paper is as follows. In section 2, we construct an FEM model of crane-hook and introduce the Load-Deformation (L-D) database. This database is prepared by using the FEM model; it is constructed as a collection of the applied load conditions and the corresponding deformed node positions. In section 3, we explain the image processing procedure to detect the feature points from the failed crane-hook images. In section 4, we develop the identification method of load condition based on our evaluation criterion. We introduce the EM algorithm for the arrangement of the identification results. In section 5, we apply our estimation approach to the actual failed crane-hooks. The estimation results are represented by the form of probability distribution. In section 6, we deal with a design approach that is based on estimated load condition obtained by means of examination of the failed structures. Some concluding remarks are expressed in section 7.

2. Crane-hook Model and Load-deformation Database

2.1. Crane-hook Model

We construct a finite element model of the crane-hook based on one of its actual designs. Figure 3 shows the design drawing of the crane-hook adopted as the reference. Its cross-sectional shapes are illustrated by

Figure 1. Excavator with crane-hook and its close-up.

Figure 2. Typical crane-hook and failed sample.

the shaded area at two positions. One is the lowest center position “D” where the load is applied in the typical suspension work. The other is the position “C” where the largest stress occurs in the typical work. This area is usually called “critical section”. These cross-sectional shapes, called “T shape”, have been achieved by expert engineers empirically. Figure 4 shows the conceptual finite element model based on one dimensional beam element and the constructed model of crane-hook based on the actual design shown in Fig. 3. As indicated in Fig. 4, the latch part is omitted in the adopted model because it does not contribute to support the applied load. Each element is constructed by N_d layered as shown in Fig. 4(b). The height of cross-section is indicated by the variable “h”. The height of each layer is assigned evenly. The width of each layer is specified by “b_i” ($i = 1, \cdots, N_d$). By changing these widths b_i, we can represent various cross-sectional shapes. The analysis model is constructed of N_e elements.

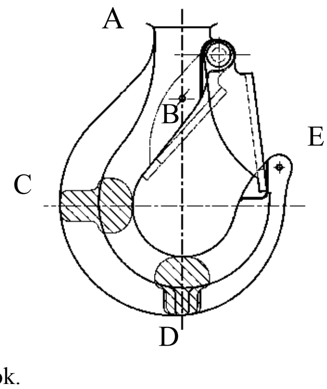

Figure 3. Design drawing of crane-hook.

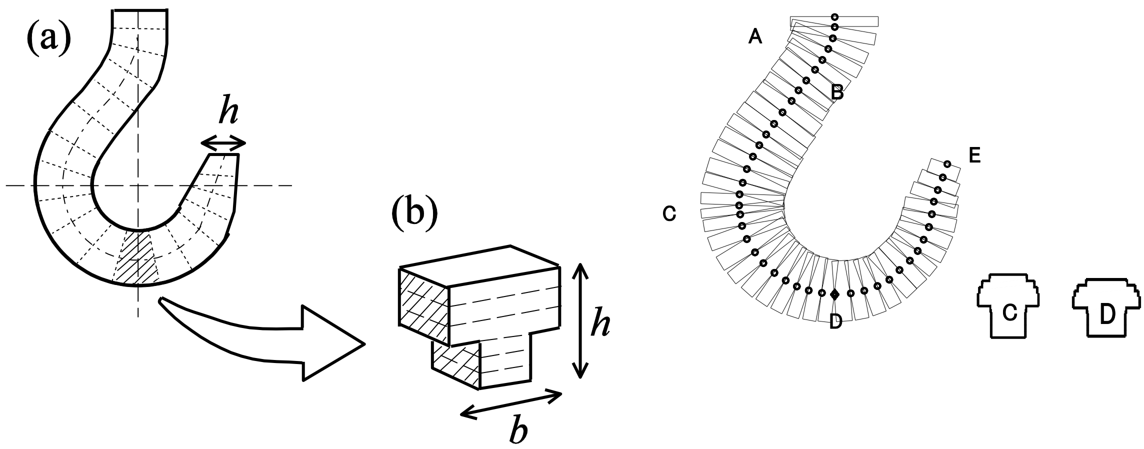

Figure 4. FE model based on 1-D beam element and constructed model referring the design drawing.

In the linear elastic deformation analysis, the equilibrium equation is obtained by means of the conventional analysis approach and expressed as

$$\boldsymbol{F} = \boldsymbol{K}\boldsymbol{U} \tag{1}$$

where $\boldsymbol{F}$, $\boldsymbol{K}$ and $\boldsymbol{U}$ are the external force vector, the stiffness matrix and the displacement vector. Given a specified external force vector and boundary conditions, the corresponding deformation of the structure is calculated on the basis of Eq. (1). In order to adapt the FEM model to the permanent deformation, we introduce an elasto-plastic deformation analysis. In our analysis, the stress-strain relationship of the material is approximated by a piecewise linear function as shown in Fig. 5. In this figure, E_1 is the Young's modulus, E_2 is the tangent modulus and $\overline{\sigma}$ is the yield stress. The dashed line indicates the relationship in the unloading process; the tangent modulus is assumed to be equal to the Young's modulus E_1 . In order to calculate the displacement of finite element model, we utilize the incremental solution scheme (Crisfield, 1991). The incremental formulation is expressed as

$$\Delta\boldsymbol{F} = \boldsymbol{K}_t \Delta\boldsymbol{U} \tag{2}$$

where $\Delta\boldsymbol{F}$, $\boldsymbol{K}_t$ and $\Delta\boldsymbol{U}$ are the incremental force vector, the tangent stiffness matrix and the incremental displacement vector, respectively. The tangent stiffness matrix $\boldsymbol{K}_t$ takes over the role of the stiffness matrix in elastic analysis. It relates small change in force to small change in displacement. The matrix $\boldsymbol{K}_t$ takes the form

$$\boldsymbol{K}_t = \boldsymbol{K}_t(\boldsymbol{U}),\ \boldsymbol{K}_t(\boldsymbol{0}) = \boldsymbol{K} \tag{3}$$

where $\boldsymbol{K}$ is the elastic stiffness matrix used in the linear elastic analysis as Eq. (1). The total displacement is computed by the sum of the incremental displacements.

$$\boldsymbol{U} = \sum_j \Delta \boldsymbol{U}_j \tag{4}$$

In the assessment process of the yielding, we utilize the layered approach (Owen and Hinton, 1980). In this approach the beam element is subdivided into layers, as shown in Fig. 4. A layer element is determined to be in yield state as a whole in the case that the central stress of the layer reaches the material yield stress. The stiffness values of the elements are determined according to the relationship shown in Fig. 5.

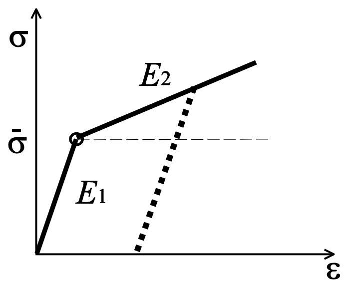

Figure 5. Adopted stress-strain relationship model.

2.2. Estimation of Physical Parameters

As shown in Fig. 5, the stress-strain relationship has the three parameters: Young's modulus E_1, tangent modulus E_2 and yield stress $\bar{\sigma}$, which must be determined. We estimate them based on experimental data. The stretch experiment of crane-hooks conducted is as follows. A load is applied at the point "D" of crane-hook shown in Fig. 3. We measure the distance between points "B" and "E" at various load magnitude and calculate the enlargement of the distance. Figure 6 shows the obtained experimental result. The ordinate and the abscissa represent the magnitude of load [kN] and the enlargement of distance between point "B" and "E" [mm], respectively. On the basis of the obtained data, the plastic deformation begins to be observed at a load around 120 [kN]. The nominal load of the crane-hook dealt with in this study is 29 [kN], thus we can see that the nominal load is included in the elastic deformation area. In order to determine the material parameters based on the experimental data, we formulate a minimum square error problem as follows:

$$\text{Minimize } \sum_i (y_i - \hat{y}_i)^2 \quad \text{with respect to } E_1, E_2, \bar{\sigma} \tag{5}$$

In the above equation, y_i is the enlargement between "B" and "E" for the i th load magnitude in the result of stretch experiment. The symbol $\hat{y}_i$ indicates the enlargement obtained by the FEM analysis for the same load magnitude. Table I shows the range of these parameters and the results of the error-minimization. The results are obtained by the exhaustive search and are shown in the lowest row. In the following, we utilize these estimated values for the FEM analysis.

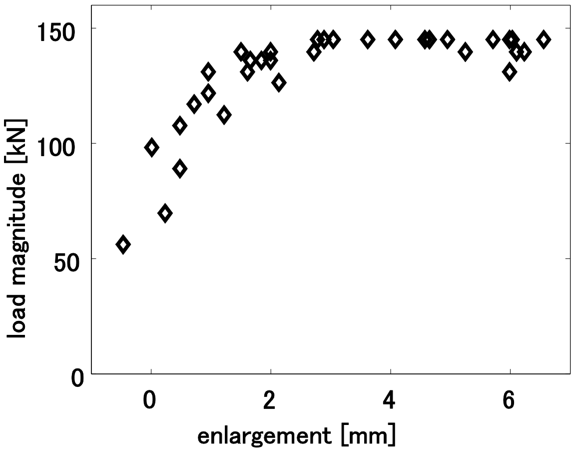

Figure 6. Relation between applied load and enlargement of displacement.

Table I. Range of parameters and results of error-minimization

	E_1 [GPa]	E_2 [GPa]	$\bar{\sigma}$ [MPa]
range	180 ~ 280	0.1 ~ 50	100 ~ 400
estimated	260	1	200

2.3. CONSTRUCTION OF L-D DATABASE

The Load-Deformation (L-D) database is a collection of data; the various load conditions and the corresponding information of deformation are recorded. In the current study, the L-D database is designed to have the following information obtained by the FEM analysis:

- analysis number
- applied load condition on the FEM model
  - load applied node
  - load magnitude
  - load direction
- deformed node positions

We explain the contents of L-D database concretely. Figure 7 shows the load applied nodes and load directions. The FEM model consists of 42 elements and 43 nodes. The load applied nodes are 9 nodes from 21th node to 37th node; the list of node is $[21, 23, 25, 27, 29, 31, 33, 35, 37]$. The load direction is considered 7 direction patterns from -180° (leftward) to 0° (rightward); -90° corresponds to the vertical direction. These direction vectors are defined in a global coordinate system. The load magnitude is prepared from 20[kN] to 140[kN] with an interval of 20[kN]. The ratio of these magnitudes to the nominal load is from 0.69 to 4.82. The load magnitude is 7 patterns and the list is [20, 40, 60, 80, 100, 120, 14] [kN]. The pattern of all combination is 441 and all calculation results are recorded in the L-D database as the form of deformed node positions. The estimation of the load condition is performed based on the deformed node positions in the L-D database.

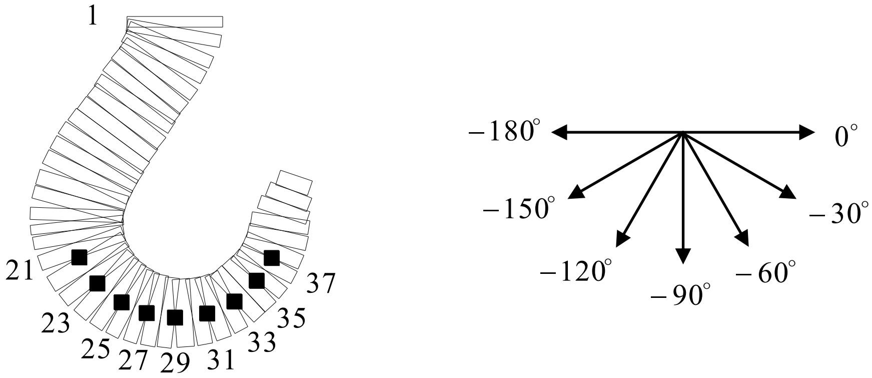

Figure 7. Load conditions; load applied nodes and load directions.

3. Feature Points Detection from Crane-hook Images

In this section, we explain the detection process of hook deformation from the failed hook image. The deformation of a failed crane-hook is represented based on the feature points detected from the failed image. The selection of feature points is performed by means of the digital image processing. This section consists of two parts. In the former part, we introduce the procedure of image processing used in this study. The outline of crane-hook is obtained from the failed hook image. In the latter part, we discuss the detection algorithm of feature points. The feature points are identified based on the obtained outline image.

3.1. Preprocessing of Crane-hook Image

The digital image of a failed hook is processed to obtain its shape outline. Figure 8(a) shows a typical example of failed hook image. This figure is displayed with a 256 step gray scale. Figure 8(b) is obtained by applying the digital image processing to Fig. 8(a). If there are some line gaps, we modify the outline through manual operations. Figure 8(c) shows the outline image without the latch part. The removing of latch part and the interpolation of line gap is performed by manual operations. In Fig. 8(c), the tip-end and the base positions are indicated by the circle and the arrow, respectively. The details are explained in our previous work (2012).

3.2. Detection Process of Feature Points

The detection process of feature points is consists of two steps. The first step is the determination of boundary line between the inner area and the outer area. The second step is the selection of the feature points on the boundary line. As the preparation of the first step, the outline is divided into two parts; one is the inner outline and the other is the outer outline. By following the outline from the tip-end point, the inner outline at the upper side and the outer outline at the lower side are determined. In order to determine the

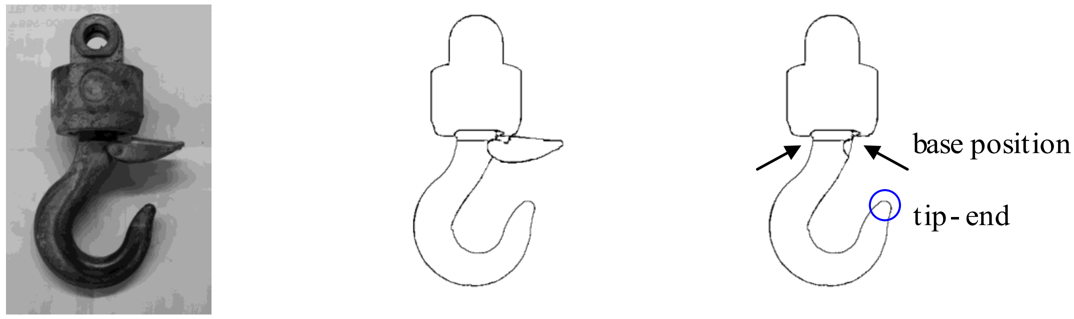

(a) Gray scale image (b) Filtered outline image (c) Outline image (without latch part)

Figure 8. Processed images.

boundary line, we utilize the dilation process of the outlines. In each cycle of dilation process, the same label that distinguishes between the inner area and the outer area is assigned to the adjacent pixels of the outlines. Figure 9(a) shows the result of 5 cycles of dilation process. The outer outline is represented darker and the inner outline is represented lighter. By repeating the dilation process until the inner and outer areas collide, the boundary between the inner area and the outer area is obtained. Figure 9(b) shows the boundary line obtained by the dilation process. The feature points are detected on this boundary line. The boundary line is divided into N_f sections evenly. The division points are selected as the feature points and they are represented by the symbol '$\times$' in Fig. 9(c).

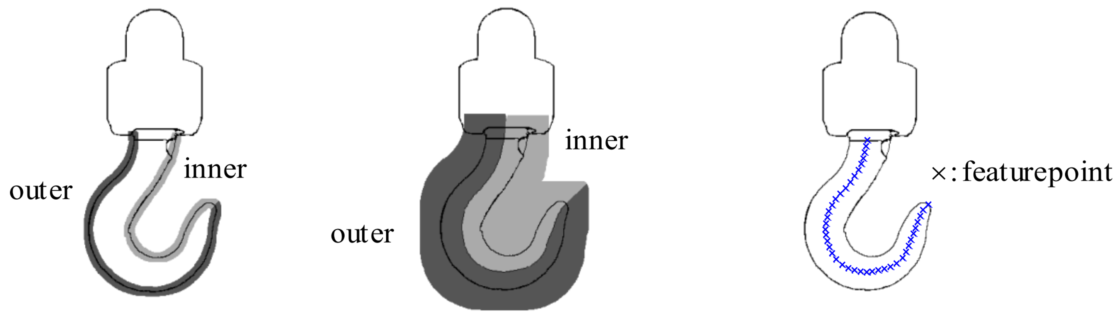

(a) Dilation of outline (b) Boundary of inner and outer area (c) Detected feature points

Figure 9. Detection process of feature points.

4. Identification Method of Load Condition

The load condition of a failed crane-hook is identified by using the L-D database. In this section, we explain the criterion used in the identification process. In the latter part, we introduce the EM algorithm that is used in the load estimation.

4.1. GEOMETRIC MOMENT

Generally, the coordinate systems used in the FEM analysis do not necessarily coincide with the coordinates used in the image processing. The shape of crane-hook should be expressed in a shape representation that is insensitive to the coordinate transformation. In this study, we turn our attention to the geometric moment of the shape. The geometric moment plays important role in object recognition and shape analysis (Ghorbel et al, 2005). The shape of hook can be described quantitatively by using geometrical moments, such as the mean, variance, and higher-order moments. The mean corresponds to the geometrical center of the shape. *n*th moments are expressed as

$$m_{pq} = \frac{1}{M}\sum_{i=1}^{M}(x_i - \bar{x})^p (y_i - \bar{y})^q, \quad p + q = n, \tag{6}$$

where p and q are degrees of power. The pair of x_i and y_i represents the coordinates of the deformed node positions in the L-D database or those of the feature points in the failed hook image. These values are normalized in terms of the base length of crane-hook. The constant M is the number of FE nodes or the feature points on the boundary line. The quantities $\bar{x}$ and $\bar{y}$ are calculated as follows:

$$\bar{x} = \frac{1}{M}\sum_{i=1}^{M} x_i \quad , \quad \bar{y} = \frac{1}{M}\sum_{i=1}^{M} y_i \tag{7}$$

We represent the information of geometric moment as a vector form. The geometric moment vector is defined as

$$\boldsymbol{m} = \begin{bmatrix} m_{10} & m_{01} & \cdots & m_{0n} \end{bmatrix}^T . \tag{8}$$

The moment vector obtained from the node positions in the L-D database is represented as '${}^{LD}\boldsymbol{m}^{(i)}$', where the superscript (*i*) indicates the analysis number in the L-D database. The moment vector obtained from the feature points based on a failed hook image is represented as ${}^{IM}\boldsymbol{m}$.

4.2. IDENTIFICATION PROCESS OF LOAD CONDITION

The data search process in the L-D database is performed based on the following evaluation function:

$$e = ({}^{LD}\boldsymbol{m}^{(i)} - {}^{IM}\boldsymbol{m})^T \boldsymbol{W} ({}^{LD}\boldsymbol{m}^{(i)} - {}^{IM}\boldsymbol{m}) \tag{9}$$

where $\boldsymbol{W}$ is the weighting factor matrix. This function evaluates the similarity of the geometric moment between the deformed node positions and the feature points of the failed hook image. In this study, we evaluate the geometric moment up to the 3rd order. The weighting factor matrix $\boldsymbol{W}$ is expressed as

$$\boldsymbol{W} = \mathrm{diag}\begin{bmatrix} 10 & 10 & 1 & 1 & 1 & 0.1 & 0.1 & 0.1 & 0.1 \end{bmatrix}. \tag{10}$$

We attach importance to the lower order moment; these values are determined empirically. The identification process is expressed as the following minimization problem:

$$\text{Minimize} \quad e \qquad \text{with respect to} \quad i, \tag{11}$$

where i is the analysis number of the L-D database. By finding the solution, we can know the applied load condition, that is, the load applied node, the load magnitude and the load direction.

4.3. EM ALGORITHM

A variety of load conditions can be obtained from the estimation process of load condition. In addition to the variety of load conditions, the quality of the estimation process can be uneven. In order to discuss the variety and the uncertainty together, we summarize the estimated results in the form of statistical representation. The representation is implemented in the form of probability distribution. In the implementation process, we utilize the EM algorithm (McLachan and Krishnan, 1997). EM (Expectation Maximization) is an iterative optimization method to estimate some unknown parameters $\boldsymbol{\Theta}$ from the given measurement data $\boldsymbol{\chi}$. However, we are not given some "hidden" nuisance variables $\boldsymbol{G}$, which need to be integrated out. We maximize the posterior probability of the parameters $\boldsymbol{\Theta}$ given the data $\boldsymbol{\chi}$, marginalizing over $\boldsymbol{G}$:

$$\boldsymbol{\Theta}^* = \underset{\Theta}{\operatorname{argmax}} \sum_{\boldsymbol{G}} P(\boldsymbol{\Theta}, \boldsymbol{G} \mid \boldsymbol{\chi}) \tag{12}$$

We can search for a maximum of $P(\boldsymbol{\Theta}, \boldsymbol{G} \mid \boldsymbol{\chi})$ by means of the following algorithm:

1. step E: calculate $P(\boldsymbol{\Theta}^{\text{old}}, \boldsymbol{G} \mid \boldsymbol{\chi})$
2. step M: $\boldsymbol{\Theta}^{\text{new}} = \underset{\Theta}{\operatorname{argmax}} \sum_{\boldsymbol{G}} P(\boldsymbol{\Theta}^{\text{old}}, \boldsymbol{G} \mid \boldsymbol{\chi}) \ln P(\boldsymbol{\Theta}, \boldsymbol{G} \mid \boldsymbol{\chi})$

In the current study, the probability density functions of the random variables are assumed to be a mixture of Gaussian distribution. This probability function consists of a linear combination of Gaussian distributions and is expressed as

$$P(\boldsymbol{\chi}) = \sum_{k=1}^{K} \pi_k N(\boldsymbol{\chi} \mid \boldsymbol{\mu}_k, \boldsymbol{V}_k), \quad 0 \le \pi_k \le 1, \quad \sum_{k=1}^{K} \pi_k = 1, \tag{13}$$

$$N(\boldsymbol{\chi} \mid \boldsymbol{\mu}, \boldsymbol{V}) = \frac{1}{(2\pi)^{D/2} |\boldsymbol{V}|^{1/2}} \exp\{-\frac{(\boldsymbol{\chi} - \boldsymbol{\mu})^T \boldsymbol{V}^{-1} (\boldsymbol{\chi} - \boldsymbol{\mu})}{2}\}, \tag{14}$$

where π_k, $\boldsymbol{\mu}, \boldsymbol{V}$ and D are the mixture weights, the mean, the variance and a number of dimension, respectively. The parameter vector $\boldsymbol{\Theta}$ is denoted by $\boldsymbol{\Theta} = [\pi_k, \boldsymbol{\mu}_k, \boldsymbol{V}_k]$. In this case, the EM algorithm is represented as follows:

1. initialize the parameters, π_k, $\boldsymbol{\mu}_k$ and $\boldsymbol{V}_k$
2. step E: calculate

$$\gamma(z_{nk}) = \frac{\pi_k N(\boldsymbol{\chi}_n \mid \boldsymbol{\mu}_k, \boldsymbol{V}_k)}{\sum_{j=1}^{K} \pi_j N(\boldsymbol{\chi}_n \mid \boldsymbol{\mu}_j, \boldsymbol{V}_j)} \tag{15}$$

3. step M: calculate

$$\boldsymbol{\mu}_k^{\text{new}} = \frac{1}{N_k} \sum_{n=1}^{N} \gamma(z_{nk}) \boldsymbol{\chi}_n \tag{16}$$

$$\boldsymbol{V}_k^{\text{new}} = \frac{1}{N_k} \sum_{n=1}^{N} \gamma(z_{nk})(\boldsymbol{\chi}_n - \boldsymbol{\mu}_k^{\text{new}})(\boldsymbol{\chi}_n - \boldsymbol{\mu}_k^{\text{new}})^T \tag{17}$$

$$\pi_k^{\text{new}} = \frac{N_k}{N} \tag{18}$$

After the convergence of this algorithm, we can determine the probability distribution of load condition.

5. Estimation Results

5.1. Identification of Load Condition Using Stretch Test Image

In order to confirm the effectiveness of the implemented estimation approach, we apply the method to a deformed hook image obtained by means of the stretch experiment. Figure 10(a) shows the initial state image of crane-hook. Figure 10(b) shows the deformed state image. A downward load (140 [kN]) is applied around the point ‘D’. We can see that the contact point around the tip-end moves slightly leftward. Figure 10(c) shows the outline image of deformed hook. The latch part is excluded by manual operations. The feature points are detected from this image and the geometrical moment of this image is calculated based on the feature points. The solution of the minimization problem (11) is searched in the L-D database. The estimated load condition is shown in Fig. 11.

Comparing the estimated result with the actual applied load, the load applied point and the load direction of the estimated result shift leftward and the load magnitude is smaller than the applied load. Because of the width of loading device, the estimation problem has some difficulty for the proper identification of load condition. It should be noted that each of the estimated results is expressed to have the uncertainty to this level.

5.2. Sample Result of Load Estimation

In this part, we show a sample result of load identification. We use the failed hook shown in Fig. 8(a). The detected feature points are shown in Fig. 9(c). The identification result is shown in Fig. 12. The load applied position shifts rightward from the lower center. The load magnitude is three times greater than the nominal load. The load direction shifts rightward. The obtained result indicates that great rightward force is placed on the rightward position from the lower center.

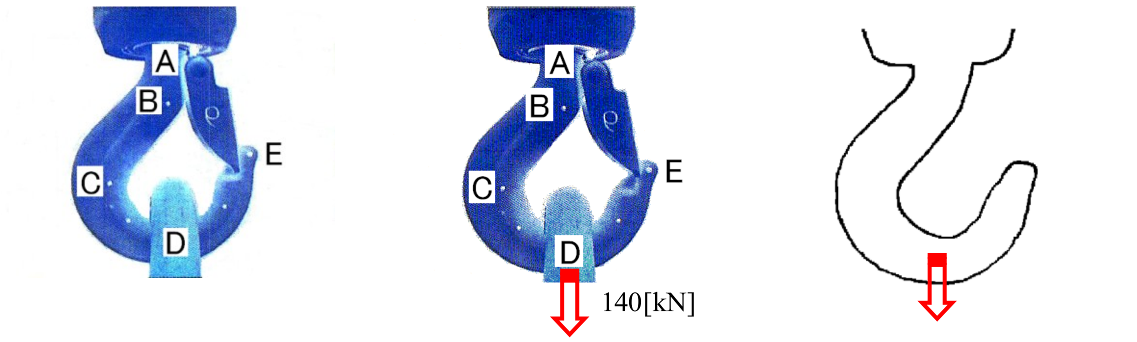

(a) Initial state (b) Deformed hook (c) Outline image of deformed hook

Figure 10. Crane-hook images of stretch experiment.

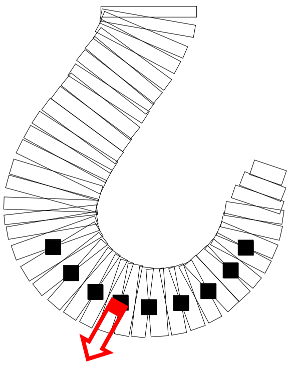

load applied node: 27
load magnitude: 100 [kN]
load direction: $\frac{4}{3}\pi$

Figure 11. Estimated loading condition using the stretch experiment image in Fig. 10.

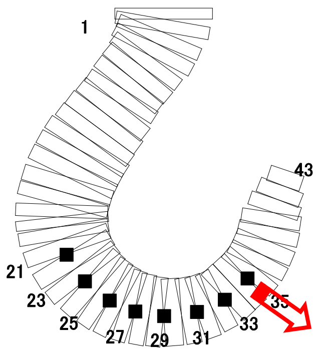

load applied node: 35
load magnitude: 100 [kN]
load direction: $\frac{5}{3}\pi$

Figure 12. Estimated loading condition using failed hook image (Fig. 8(a)).

5.3. IDENTIFICATION RESULT USING EM ALGORITHM

We apply the identification method to 12 failed samples. The probability distribution is obtained from the identified load conditions. In the current study, the number of samples is not enough to estimate the probability distribution on 3 load components (the load applied node, the load magnitude and the load direction) simultaneously. In this study, the probability distribution of each load component is treated independently. The probability distribution of each load component is expressed by a mixture of Gaussian distribution individually.

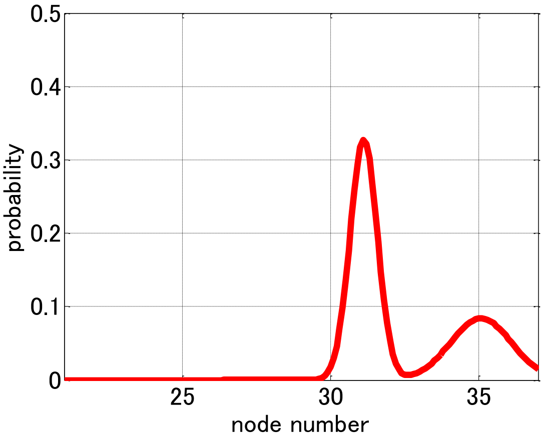

(a) Load applied node

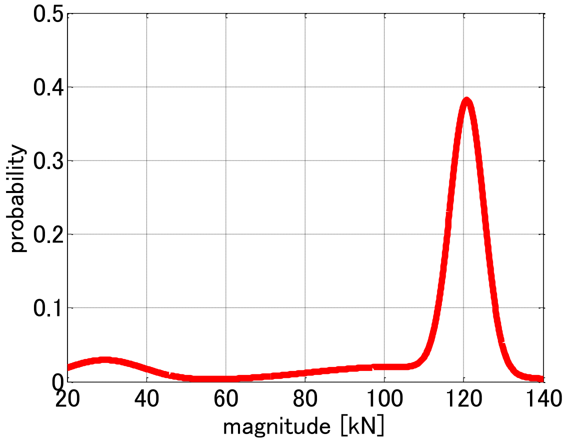

(b) Load magnitude

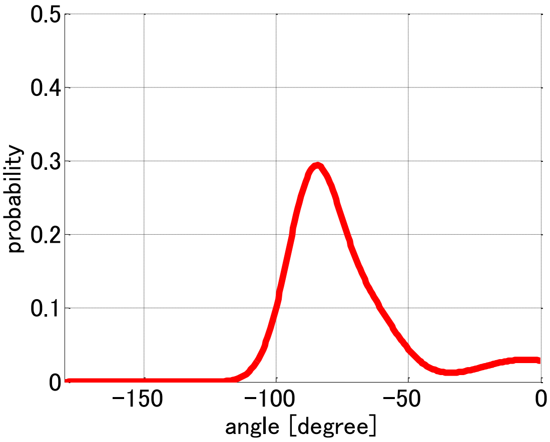

(c) Load direction

Figure 13. Probability distribution of the mixture Gaussian distribution for each load component.

Figure 13 shows the obtained results. Figure 13(a) is the distribution of load applied node. The abscissa indicates the node number. This graph has two peaks. One is sharp peak around node 31 and the other is dull curve around node 35. The distribution of load applied node has high probability at the two positions and the highest probability occurs at 31th node. Figure 13(b) is the distribution of load magnitude.

The abscissa indicates the load magnitude. This graph has one peak at 120[kN]. This value is 4 times greater than the nominal load of this hook. Figure 13(c) is the distribution of load angle. The abscissa indicates the load angle. This graph has a mild peak between -50° and -100°. The load direction tends to concentrate around downward direction. In the current study, because the load component is treated independently, we cannot show a correlation among the load components. Combining the individual results, we can see that a great load is applied at rightward position from lower center and the load direction is downward.

Figure 14 shows the estimated load applied position and the load direction. We illustrate the probability by gray-scale level based on the obtained probability distribution shown in Fig. 13(a) and (c). The high probability area is represented darkly, whereas the low probability area is represented lightly. The darkest region and arrow in Fig. 14 is the most probable area and the direction when crane-hooks are failed.

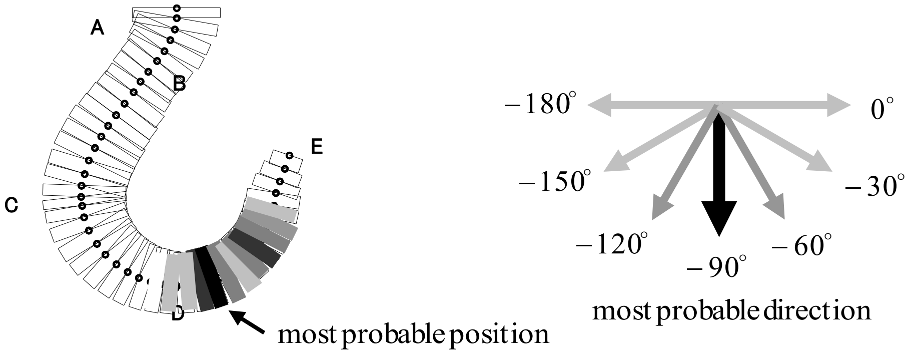

Figure 14. Estimated load applied position and load direction.

6. Optimal Design

6.1. Design Variables and Their Parametric Representation

In this study, the design variables of crane-hook are the parameters of cross-section of beam elements. As shown in Fig. 4, the parameters are the height and layer widths. These design variables are represented as functions of the local coordinate s attached at the center line of hook, as $h(s), b_i(s)$ $(0 \leq s \leq L)$, where L is the length of the contour line. The coordinate s is indicated in Fig. 15. The start point of s is the base point "A" and the end point is the tip point "E". In the followings, $h(s)$ and $b_i(s)$ are called the shape functions.

We represent such shape functions as linear combination of the Gaussian function. The shape functions are then expressed as

$$h(s) = \sum_{j=1}^{N_h} \alpha_j^h \exp\left(-\frac{(s-\mu_j^h)^2}{2(\beta_j^h)^2} \right) \tag{19}$$

$$b_i(s) = \sum_{j=1}^{N_b} \alpha_j^{b_i} \exp\left(-\frac{(s-\mu_j^{b_i})^2}{2(\beta_j^{b_i})^2} \right) \tag{20}$$

where α is the scaling factor, μ and β are the location of the peak and the standard deviation. The constants N_h and N_b are the number of Gaussian functions representing h and b_i, respectively. By introducing this representation, the shape functions $h(s)$ and $b_i(s)$ are represented in terms of the coefficients $\alpha_j^h, \beta_j^h, \mu_j^h$ $(j=1,\cdots,N_h)$ and $\alpha_j^{b_i}, \beta_j^{b_i}, \mu_j^{b_i}$ $(j=1,\cdots,N_b)$.

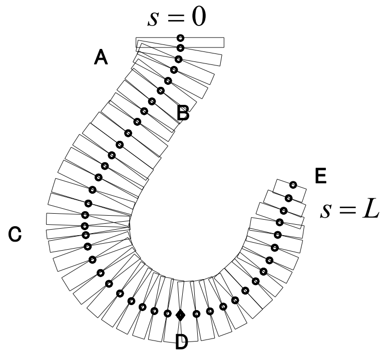

Figure 15. Local curvilinear coordinate s .

6.2. SETTING OF CRITERIA AND FORMULATION OF OPTIMIZATION PROBLEM

We explain the formulation of criteria that evaluate the goodness of crane-hook design. In order to improve the performance of crane-hook, we employ the following criteria:
– structural weight
– structural stiffness

The first criterion is selected for achievement of lightweight. The lightweight is important for the saving of material cost and the compactness. The structural weight J_1 is formulated as

$$J_1 = \sum_{i=1}^{N_e} \rho A_i l_i \tag{21}$$

where ρ is the material density, A_i is the cross-sectional area of i -th element and l_i is the element length.

The second criterion is selected for the evaluation of the robustness of structure against unspecified multiple load conditions. For this evaluation, we adopt the ratio between the norm of the global displacement vector and the norm of the possible load vector. The robustness of the structure is evaluated in terms of the maximum value of the ratio. The possible load vector is represented by $\tilde{\boldsymbol{F}}$. This vector specifies the possible load applied points and respective components based on the estimation result. We utilize the estimation result of the load applied node discussed in the previous section. The maximum ratio is expressed as

$$\max_{\tilde{\boldsymbol{F}}\neq 0}\frac{\|\boldsymbol{U}\|}{\|\tilde{\boldsymbol{F}}\|} \tag{22}$$

$$\boldsymbol{U}=\boldsymbol{K}^{-1}\boldsymbol{F} \quad \text{where} \quad \boldsymbol{F}=\boldsymbol{B}_v\tilde{\boldsymbol{F}} \tag{23}$$

where $\|\bullet\|$ represents the vector norm and $\boldsymbol{K}$ is the elastic stiffness matrix in Eq. (1). The global force vector $\boldsymbol{F}$ is associated with the possible load vector $\tilde{\boldsymbol{F}}$ by the weight factor matrix $\boldsymbol{B}_v$. The component value of the matrix $\boldsymbol{B}_v$ is specified according to the probability distribution of load applied node shown in Fig. 13(a). The maximum ratio is rewritten as the following form.

$$\max_{\tilde{\boldsymbol{F}}\neq 0}\frac{\|\boldsymbol{U}\|}{\|\tilde{\boldsymbol{F}}\|}=\max_{\tilde{\boldsymbol{F}}\neq 0}\frac{\|\boldsymbol{K}^{-1}\boldsymbol{F}\|}{\|\tilde{\boldsymbol{F}}\|}=\max_{\tilde{\boldsymbol{F}}\neq 0}\frac{\|\boldsymbol{K}^{-1}\boldsymbol{B}_v\tilde{\boldsymbol{F}}\|}{\|\tilde{\boldsymbol{F}}\|} \tag{24}$$

The magnitude of $\|\tilde{\boldsymbol{F}}\|$ is normalized to be 1. Here, instead of searching the maximum value directly, we utilize the matrix norm. According to the maximum principle of the eigenvalue, the maximum value of this function is calculated as the matrix norm induced by the Euclidean vector norm $\|\bullet\|_2$ (Roger and Charles, 1985). The second criterion is formulated as

$$J_2=\|\boldsymbol{K}^{-1}\boldsymbol{B}_v\|_2=\max\left\{\sqrt{\lambda}:\lambda\ \text{is an eigenvalue of}\ (\boldsymbol{K}^{-1}\boldsymbol{B}_v)^T(\boldsymbol{K}^{-1}\boldsymbol{B}_v)\right\}. \tag{25}$$

This criterion represents a displacement-force ratio and the unit is [m/N].

We formulate the criteria to be minimized in the above. For this multi-objective optimization problem with the two items, an integrated evaluation function is introduced in terms of the weighting factors. The multi-objective optimal design problem of the crane-hook is then expressed as follows:

$$\begin{array}{ll} \text{Minimize} & J = \gamma_1\dfrac{J_1}{\underline{J_1}}+\gamma_2\dfrac{J_2}{\underline{J_2}} \equiv \gamma_1\tilde{J}_1+\gamma_2\tilde{J}_2 \\ \text{with respect to} & \boldsymbol{x} \\ \text{subject to} & h_L\le h(s)\le h_U,\ b_L\le b_i(s)\le b_U,\ \gamma_1+\gamma_2=1 \end{array} \tag{26}$$

where $\boldsymbol{x}=\lfloor \alpha_j^h \quad \beta_j^h \quad \mu_j^h \quad \alpha_j^{b_i} \quad \beta_j^{b_i} \quad \mu_j^{b_i} \rfloor$ $(i=1,\cdots,N_d,\ j=1,\cdots,N_h\ \text{or}\ N_b)$. The constants $\underline{J_1}$ and $\underline{J_2}$ are the evaluation item values for normalization. We adopt the FEM model of crane-hook shown in Fig. 4, called "reference design", for this normalization. The values $\underline{J_1}$ and $\underline{J_2}$ are calculated for the reference design. The coefficients γ_1 and γ_2 are the weighting factors for the criteria. We conduct the optimal designs under the various combinations of the weighting factors. In the constraint conditions, h_L, b_L and h_U, b_U are the lower and upper bounds of the height and width.

6.3. SETTING OF PARAMETERS FOR NUMERICAL CALCULATION

The optimization problem (26) is solved by means of the particle swarm optimization (PSO). The PSO is one of the population-based stochastic optimization techniques and has been successfully applied in many research and application areas (Behera and Choukiker, 2010; Mauro et.al., 2009). In the PSO, we need to specify the number of particles and the number of iterations. These parameters are shown in Table II(a). The values of the material parameters E_1, E_2 and $\bar{\sigma}$ are same as the determined values in section 2.2. The parameters of finite element model are shown in Table II(b). The constants in Eq. (26) are specified in Table II(c). The evaluation item values obtained based on the reference design are as follows:

- structural weight $\underline{J_1}$: 2.660 [kg]
- structural stiffness $\underline{J_2}$: 1.4083×10^{-7} [m/N].

The adopted weighting factors in Eq. (26) are specified as

$$\gamma_i = \{0.0, 0.05, 0.10, \cdots, 0.90, 0.95, 1.00\} \quad (i = 1, 2)\,. \tag{27}$$

Table II. Parameters for numerical calculation

	Item	Symbol	Value
(a) Finite element model	Material density	ρ	7.87 [g/cm^3]
	Number of elements	N_e	40
	Number of layers	N_d	10
(b) Optimization problem	Number of Gaussian	N_h, N_b	4
	Lower bound of size	h_L, b_L	5 [mm]
	Upper bound of size	h_U, b_U	40 [mm]
(c) PSO	Number of particles		1000
	Number of iteration		100

6.4. OBTAINED OPTIMAL DESIGNS

Figure 16 shows the distribution of the criterion function values of the solution of the optimization problem (26). The abscissa shows the structural weight $\tilde{J}_1$ and the ordinate shows the structural stiffness $\tilde{J}_2$. Each item value indicates the ratio to the value of reference design. It can be seen that the Pareto line is constructed by the obtained solutions. From the results in this figure, there is a trade-off relationship among the evaluation items. Respective shapes concerning to the solutions (A) and (B) on the Pareto line in Fig.16 are shown in Fig. 17. The evaluation item values are indicated in the caption. In Fig. 17(a) and (b), the left part shows the height distribution of the elements. In the following, we call this part as “hook shape”. The right part shows the selected cross-section of the design solution; the upper is the section of the point “C” (17th element) and the lower is that of the lowest center point “D” (29th element). The top and bottom of the section shape correspond to the inner and outer surfaces of the hook, respectively. These two are important sections in the practical design scene.

The following features are observed for the obtained hook shape:

– hook shape becomes thinner toward the tip point “E” from the lowest center point “D”
– thickness of region around the point “B” is greater than any other region

If the attached importance on “the structural weight J_1 ” is larger, the first feature becomes more remarkable. Because the stresses on the surface of hook between the load applied point and the tip point “E” are equals 0, this part has no contribution to the strength. Tapering off around the tip point “E” is a rational shape. In both solutions, the thickest region is not the point “C” (critical section) but also around the point “B”. Because we specify the weight factor matrix $\boldsymbol{B}_v$ based on the estimation result, the possible load applied node is shifted rightward. As a result of this formulation, the most critical area shifts from the point “C” to the upward point “B”.

We discuss the feature of the cross-sectional shape. The section of the point “C” is the rectangular shape. If we attach importance to the weighting factor γ_1, the cross-sectional shape of the point “C” becomes thinner toward the bottom. The stress in the lower part is smaller than that of the upper part; thus the tapering off shape is good for the lightweight. At the point “D”, the width of section around the center part is thinner than both end side (upper and lower). In order to keep high stiffness in the unspecified load cases, it is better to thicken the bottom than to thicken the middle part.

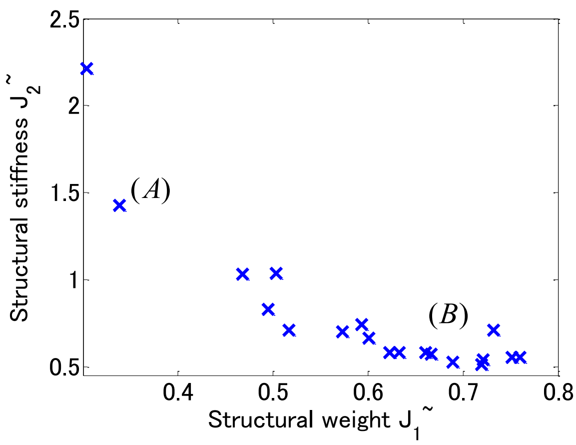

Figure 16. Distribution of objective function values for respective weighting factors.

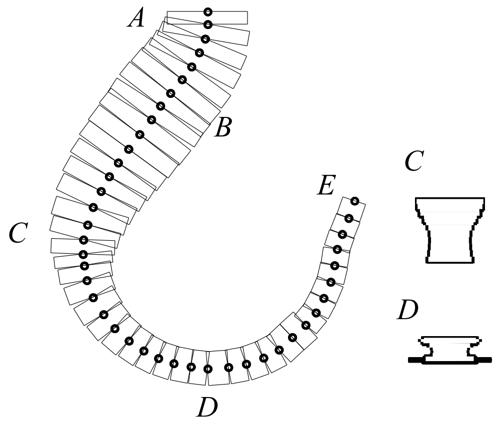

(a) Hook shape and sections of solution (A)
$(\widetilde{J}_1 = 0.3324, \widetilde{J}_2 = 1.4328)$

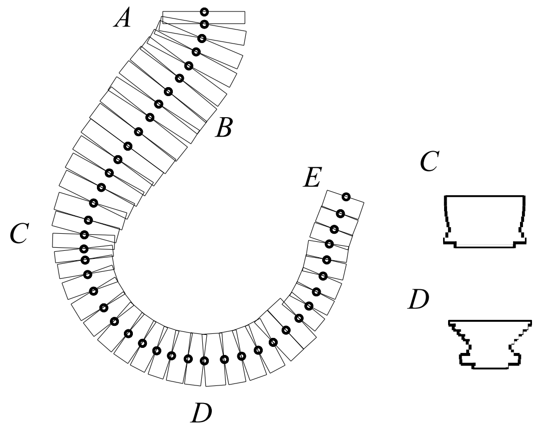

(b) Hook shape and sections of solution (B)
$(\widetilde{J}_1 = 0.6895, \widetilde{J}_2 = 0.5263)$

Figure 17. Obtained designs of crane-hook.

The key points obtained from the observation of the solutions are as follows:

- hook shape is tapering off from the lowest center point
- the region around the point “B” is thicker than any other area
- cross-sectional shape of the point “C” is rectangular
- tapering-off shape of hook becomes conspicuous as the importance is attached to the lightweight

7. Conclusion

The estimation of load condition and the optimal design of crane-hook are presented and discussed. The objective of the estimation is to find out the load condition when crane-hooks are failed. In order to adapt the FEM model to the permanent deformation, we implement elasto-plastic deformation analysis. The Load-Deformation database that has the pairs of the applied load condition for the FEM model and their deformed node positions is constructed. The feature points are detected on the failed hook image in order to compare those feature points with the deformed node positions recorded in the L-D database. The applied load condition corresponding to the failed crane-hook image is then obtained by using a difference-minimization approach. The identified loading conditions summarized individually in the form of the mixture Gaussian distribution. In the parameter estimation process on the distribution, we utilize the EM algorithm. The result is that the load applied position lies between the lowest center point and the tip-end, the load magnitude is four times larger than the nominal load and the load direction is the downward.

In order to obtain a high-quality design, we formulate the multi-objective optimization problem taking account of the estimated results. The evaluation items are the structural weight and the structural stiffness. In the representation of the design variables, we utilize the Gaussian functions. The multi-objective problem is converted into the single objective problem by introducing the weighting factors. This problem is solved by means of the PSO. The obtained crane-hook shapes have a tapered shape similar to those of actual crane-hook designs. However, there are different features on the crane-hook shape. The thickest area of the obtained shape shifts upper part than that of the actual design. The cross-sections do not have a T-shape that is implemented in the actual design but have “a rectangular shape” or “an hourglass shape”. By introducing the Gaussian function to represent the design variables, we can reduce the number of design variables and represent the shape functions effectively.

In this study, the components of load condition are estimated individually. This is because the number of failed samples is not enough to calculate the correlation among the load components. Taking the correlation into account, the failure estimation result becomes more meaningful. This is our future work.

References

Quek, S. T., Tran, V. A., Hou, X. Y. and Duan W. H. Structural damage detection using enhanced damage locating vector method with limited wireless sensors. *Journal of sound and vibration*, 38(4-5):411-427, 2009.

Lam, H. F. and Ng, C. T. The selection of pattern features for structural damage detection using an extended Bayesian ANN algorithm. *Engineering Structures*, 30(10):2762-2770, 2009.

Muromaki, T., Hanahara, K., Tada, Y. and Nishimura, T. Estimation of loading conditions of failed crane-hook: an image-based approach with knowledge and simulation. *International Journal of Reliability and Safety*, 6(1/2/3):130-147, 2012.

Crisfield, M. A. *Non-linear Finite Element Analysis of Solid and Structures: Volume 1*, John Wiley & Sons, 1991.

Owen, D. R. J. and Hinton, E. *Finite Elements in Plasticity: Theory and Practice*. Pineridge Press Limited, Chapter 5, 1980.

Ghorbel, F., Derrode, S. Dhahbi, S. and Mezhoud, R. Reconstructing With Ceometric Moments. *Int. Conf. on Machine Intelligence (ACIDCA-ICMI'05)*, Tozeur, Tunisia, November 5-7, 2005.

McLachlan, G. J. and Krishnan, T. *The EM Algorithm and Extensions*, Wiley-Interscience, 1997.

Roger, A. H. and Charles, R. J. *Matrix Analysis*, Cambridge University Press 1985.

Behera, S. K. and Choukiker, Y. Design and Optimization of Dual Band Microstrip Antenna Using Particle Swarm Optimization Technique. *Infrared Milli Terahz Waves*, 31:1346-1354, 2010.

Mauro, A. S. S. R. et. al. Optimal Design of Shell-and-Tube Heat Exchanges Using Particle Swarm Optimization. *Industrial & Engineering Chemistry Research*, 48(6):2927-2935, 2009.